HIGH TEMPERATURE THERMAL ENERGY STORAGE FOR SOLAR COOLING APPLICATIONS

Eduard Oró, Antoni Gil, Marc Medrano, Ingrid Martorell, Luisa F Cabeza

GREA Innovació Concurrent, Universitat de Lleida, Edifici CREA, Pere de Cabrera s/n, 25001 Lleida, Spain, Phone: +34 973 00 35 77, Fax: +34 973 00 35 75, E-mail: lcabeza@diei.udl.cat

Abstract

The final goal of this study is to develop a robust, compact, and efficient high temperature thermal energy storage (TES) system for solar cooling applications. A pilot plant was designed and constructed at the University of Lleida with enough flexibility to test different types of TES systems and different temperature ranges from 150 to 400 ºC. This pilot plant is already operative and has a thermal oil heater of 22 kW of power, an air heat exchanger of 20 kW, and a TES tank. All of these devices were designed by the University of Lleida, as well as all the heat transfer fluid (HTF) circuit, including valves, pipes and connections. This work is focused in the selection of the storage material, and design and construction of the storage tank.

1 Introduction

High temperature thermal energy storage (TES) may play an important role in the industrial field and in solar applications. However, before implementing a specific TES technology type [1,2], a suitable storage medium has to be selected and characterized, and some working parameters and features must be determined, which is why a pilot plant is needed to obtain such parameters experimentally. In order to reach this objective, a selection and characterization process for several storage media was undertaken, and a small scale pilot plant was designed and constructed at the University of Lleida. This pilot plant will be capable to test accurately different TES systems working with latent heat storage materials or sensible heat storage materials [3].

Solar cooling is the use of thermal solar energy to produce cold in a thermally activated cooling technology, using absorption, adsorption, or desiccant cooling technologies. The main challenge of solar cooling technologies is that solar energy is not constant in time and in power; and cold demand neither. TES can help this application by storing the heat produced in the solar collectors at a temperature range of 140-200 ºC, and releasing it at the required time, temperature and power, and by storing the produced cold at a temperature range of 5-10 ºC. The combination of solar thermal energy and TES systems improves the dispatchability and efficiency of the system. This study is focused on the first strategy of storing the heat.

The objective of this work is to design and construct a high temperature energy storage tank in order to test and characterize a storage material. The storage materials for this application are phase change materials (PCM) with a melting temperature range of 155-175 ºC. In order to carry out the thermal calculations for this design, previous experiments with low temperature phase change material (PCM) were taken in account [4].

2 Selection of the storage material

2.1 Materials

Recently, different reviews listing PCM adequate to store energy at temperatures higher than 120 ºC have appeared in the literature [1,2,5]. The first stage of the investigation was to select a temperature range adequate for heat storage in solar cooling applications. The temperature range selected was 145-185 ºC, where 185 ºC represents the temperature leaving the solar collector and 145 ºC the minimum inlet temperature in the absorption chiller. Another important requirement was an enthalpy higher than 150 kJ/kg. According to these requirements, a search and a systematic study of candidate materials to be used as PCM in the energy storage system was done.

Table 1 shows the properties of the candidate materials, selected according to the melting temperature and phase change enthalpy.

Table 1. List of materials tested with possibilities to work as PCM [6,7].

Material	CAS number	Melting temperature [ºC]	Phase change enthalpy [kJ/kg]	Material classification
Salicylic acid	69-72-7	159	199	Organic
Benzanilide	93-98-1	161	162	Organic
D-Mannitol	69-65-8	167	316	Organic
Hydroquinone	123-31-9	172.2	258	Organic
Potassium thiocyanate	333-20-0	173	280	Organic

PCM candidates were tested in our laboratories to determine the temperature ranges of melting and solidification, and the corresponding enthalpy for these ranges.

On the other hand, mechanical, chemical, economic, and environmental properties of the candidate (as volumetric variation between solid and liquid, chemical stability, vapour pressure, toxicity, compatibility with the container material, price, availability, etc) were taken into account.

2.2 Methodology of analysis

The equipment used for the analysis of the materials was a calorimeter DSC 822e. With this equipment the following properties were measured for each of the PCM candidates: temperature ranges of melting and solidification, specific heat as a function of temperature for both liquid and solid phases, and fusion and solidification enthalpies.

First of all, an analysis by dynamic method was carried out for all the materials. This method gives a first and fast approach for the above mentioned thermal properties and was used to check literature values. The more accurate but slower STEP method was applied for each substance, using very small temperature increases in the areas of phase change, to determine the ranges of temperatures and the enthalpies of melting and solidification more precisely. All samples studied have a weight of between 15.00 mg and 15.50 mg, with the aim that the results are fully comparable [8, 9].

2.3 Results of the analysis

The results obtained in these analyses are summarized in Table 2. These results are average values for the three repetitions done for each material. Average standard deviations for all the materials are below 5.76 kJ/kg for the average $\Delta H_{melting}$ and below 6.41 kJ/kg for the average $\Delta H_{solidification}$. For the average temperatures, the standard deviations are 0.23 ºC for the melting temperature and 0.57 ºC for solidification temperature.

2.4 Conclusions of the analysis tests

In this study, a material satisfying all the needs of the studied application (melting point, enthalpy value, material availability, price, chemical risks, etc.) was not found. However, three of them (benzanilide, D-mannitol, and hydroquinone) show results in accordance with the specifications of melting point and enthalpy.

Concerning to the solidification point, Table 2 shows that subcooling is present in all materials. This effect is very important in the selection of a candidate, because subcooling can bring the solidification temperature to a value below the minimum requirement temperature (145 ºC). A possible solution to avoid the subcooling

effect is the use of a nucleation agent for each PCM. Table 2 shows that salicylic acid loses large amounts of product during the test. Also, the phase change enthalpy of potassium thiocyanate is lower than the minimum established previously. Therefore these two materials were discarded.

D-mannitol showed the highest subcooling, with solidification temperatures under the minimum working temperature of the application (145 ºC). Benzanilide presented also a high and unacceptable subcooling.

Therefore, hydroquinone was chosen as a candidate as a PCM because its melting point, solidification point, and enthalpy satisfies the initial specifications.

Table 2. Summary of results obtained for the materials tested, according to the different methods.

	ΔH bibliography [kJ/kg]	ΔH of fusion DSC [kJ/kg]	ΔH of solidification DSC [kJ/kg]	Melting point bibliography [ºC]	Melting point DSC [ºC]	Solidification point DSC [ºC]
Salicylic acid	199.00	157.47	104.90	159.00	159.29	110.93
Benzanilide	162.00	138.88	129.39	161.00	163.58	136.07
D-Mannitol	316.00	261.22	214.68	167.00	166.56	116.04
Hydroquinone	258.00	235.85	187.98	172.40	172.73	158.93
Potassium tyocyanate	280.00	114.36	112.52	173.00	176.61	156.86

3 Design and experimental results of the storage tank

3.1 Design of the storage tank

The main requirements to design the storage tank were a thermal power capacity of 3-15 kW and an energy storage time of at least one hour. Different configurations of heat exchanger were considered and analysed to be used as TES tanks. A shell and tubes heat exchanger was finally selected as the most appropriate one for this application. The PCM is located in the shell part and the heat transfer fluid (HTF) circulated through the tubes. Two variations of this type of tanks were studied: one without fins and the other with fins. The fins were included to enhance heat transfer in the PCM side (Fig. 1 and Fig. 2). Design results show how thermal power increases with the number and length of the tubes and that the fins allow about a three-fold increase in heat transfer.

The tank without fins was built in the University of Lleida by GREA. Fig. 3 shows the 3-dimensional design of the energy storage tank. For a good analysis of the thermal behaviour of PCM, 27 temperature probes were installed at different locations in the tank. Fig. 3 shows the location of the temperature sensors and the nomenclature used.
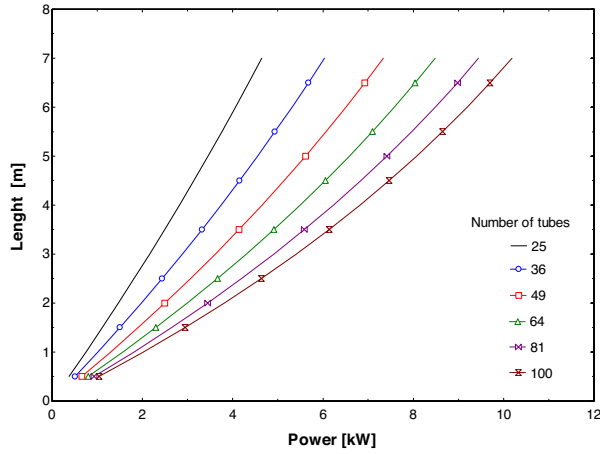
Fig. 1. Power of the storage tank without fins versus tube length and number of pipes.
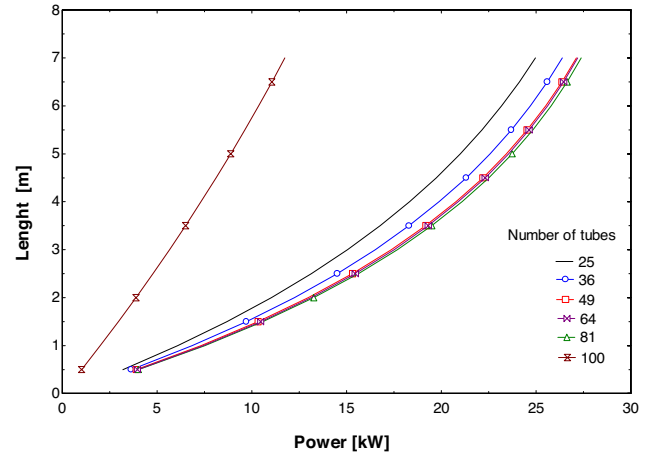
Fig. 2. Power of the storage tank with fins versus tube length and number of pipes.

The sensors were distributed in different points of the PCM tank: sensors from $T_{PCM.1}$ to $T_{PCM.15}$ are measuring the temperature of the PCM located between the HTF tubes; sensors from $T_{pla.1}$ to $T_{pla.6}$ are measuring the temperature of the PCM in the central zone of the tank; and sensors from $T_{PCM.e.1}$ to $T_{PCM.e.1}$ are measuring the temperature in the corners of the tank.
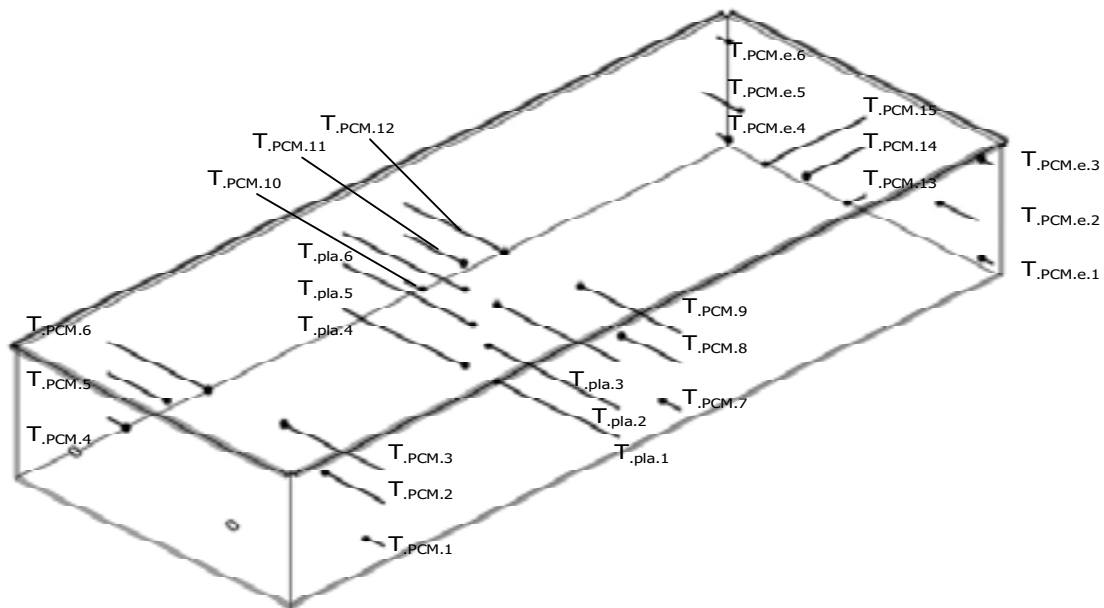

Fig. 3. Location and nomenclature of the temperature probes in the thermal energy storage tank.

3.2 Average temperature indicators

To evaluate the behaviour of the PCM in the tank, the average temperature indicators were calculated. Four different methods of calculation were studied:

- Average temperature of control volumes in all the tank (T_{CV})

- Average temperature of control volumes without corners and central zone ($T_{CV.wc\&wcz}$)

- Average temperature of control volumes of central zone ($T_{CV.cz}$)

- Average temperature of control volumes of corners ($T_{CV.c}$)

The control volumes are defined as the amount of PCM material that can be associated to every temperature sensor. These control volumes were determined according to the geometry inside the tank. Consequently, the temperature of this amount of PCM was considered to be the same as the sensor measuring it. This weighted average temperature has been calculated according to (1), considering the temperatures from $T_{PCM.1}$ to $T_{PCM.15}$, from $T_{PCM.e.1}$ to $T_{PCM.e.6}$, and from $T_{pla.1}$ to $T_{pla.6}$ (Fig. 3).

$$T_{average.volume} = \frac{\sum_{n=first}^{n=last}\left(T_n \cdot m_{control.n}\right)}{\sum_{n=first}^{n=last}\left(m_{control.n}\right)} \qquad (1)$$

where

T_n: Temperature of each sensor associated to the respective control volume [°C]

$m_{control.n}$: Mass of PCM associated to every control volume [kg], calculated with (2):

$$m_{control.n} = V_{control.n} \cdot \rho_{PCM} \qquad (2)$$

where

$V_{control.n}$: Volume of the control volume [m^3]

ρ_{PCM}: Density of PCM, obtained experimentally [kg/m^3]

The same procedure was used to calculate the other average temperatures considered. The average temperature without corners and central zone ($T_{CV.wc\&wcz}$) was calculated considering only the temperatures from $T_{PCM.1}$ to $T_{PCM.15}$ (Fig. 3). The average temperature for central zone ($T_{CV.cz}$) considered only temperatures from $T_{pla.1}$ to $T_{pla.6}$ (Fig. 3). Finally, the average temperature of corners ($T_{CV.c}$) was calculated using only temperatures from $T_{PCM.e.1}$ to $T_{PCM.e.6}$ (Fig. 3).

The idea behind these temperature averages was to provide quick information of the thermal situation of the tank, and to establish criteria to determine and compare the starting and end point of the charging and discharging processes of the experiments.

3.3 Experimental methodology

The pilot plant enables two types of tests for high temperature TES systems, namely 1) charging and discharging the PCM at constant HTF temperature, and 2) charging and discharging the PCM while the HTF is heated up or cooled down to the specified set-point. The HTF inlet TES system temperature and HTF flow rate are controllable variables. For this paper, one particular constant HTF temperature test is described.

The PCM was studied during the charging period (melting of the PCM, **¡Error! No se encuentra el origen de la referencia.**) and discharging period (solidification of the PCM).

Before the start of the experiment, a warming period was defined. During this period the PCM is heated up to the temperature of initial experiment temperature (T_{PCM}= 150 °C, **¡Error! No se encuentra el origen de la referencia.**), in order to reach an homogeneous initial state of the PCM.

Once the PCM in the tank reached the initial experiment temperature, the HTF is heated up outside of the tank to 187 °C, and when this temperature is reached, the charging process starts (**¡Error! No se encuentra el origen de la referencia.** charging period). The temperature of the HTF in the tank inlet is nearly 187 °C, with a range of +/- 2.5°C during all the charging process. This problem of high inlet temperature oscillations

is being adressed at the moment, as a more accurate control is desirable. The charging process is stopped 5 hours after the temperature sensors installed in the body of the tank show that the melting temperature (172.73 ºC) is reached. Then the charging process is stopped and the HTF is cooled outside of the tank down to 145 ºC. When this temperature is reached the discharging process starts (**¡Error! No se encuentra el origen de la referencia.**, discharging zone). During all the discharge, the HTF is introduced in the storage tank at 145 ºC. As in the charging process, discharge is stopped 5 hours after the temperature sensors installed in the body of the tank show that the temperature of solidification (172.73 ºC) is reached.

3.4   Experimental results

Fig.4 shows the temperature in different points of the storage tank, compared with the inlet HTF temperature ($T_{tank.in,j}$). All these measurement points are close to the HTF tubes, therefore they have a similar behaviour to that of the HTF. It is possible to see that during the charging process the sensors located near the tank inlet ($T_{PCM.2}$ and $T_{PCM.8}$) have finished the melting process before the sensors close to the tank outlet ($T_{PCM.5}$, $T_{PCM.11}$, $T_{PCM.14}$). During the discharging process, the same effect can be observed. One can see that $T_{PCM.5}$, which is the temperature sensor located further away from the HTF inlet, finishes melting and solidification later than all the other ones.
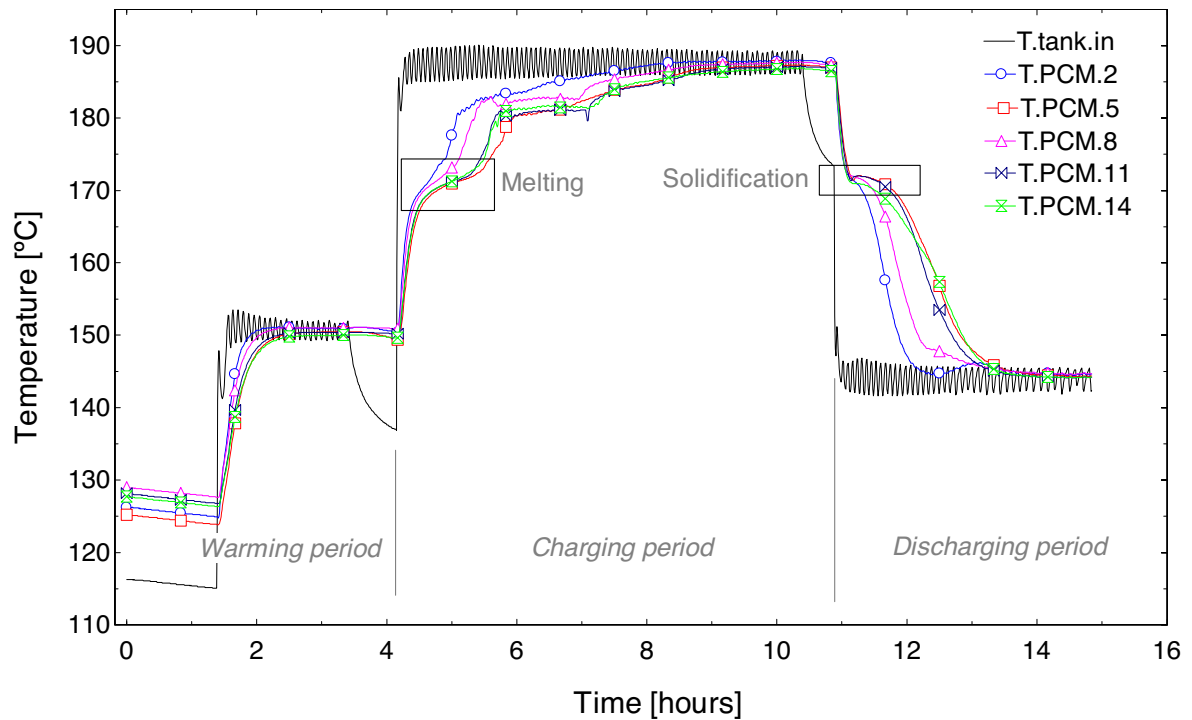

Fig. 4. Evolution of the temperature of different probes in the storage tank.

Fig. 4 shows that before the beginning of the charging process, the temperature at the inlet of the tank decreased. The same effect can be observed at the beginning of the discharge process where HTF did not flow through the tubes. When HTF flow stopped, HTF located near the inlet temperature probe started to cool down. This effect was caused by a bad insulation in the zone where the temperature sensor was installed. At the present moment this probe is correctly insulated and this effect is minimized.

Fig. 5 presents the comparison of the different average temperatures of the PCM described before. It can be observed an evident difference between the average temperatures calculated with the temperature probes located in the corners ($T_{CV.c}$) and the other three average temperatures calculated. This is due to the fact that the temperature in the corners was lower than the temperature in the rest of the tank due to the bad thermal conductivity of the PCM.

The average temperature calculated in the central zone ($T_{CV.cz}$) shows that the PCM located in this part of the

tank reached the melting point later. The average temperature in the tubes body ($T_{CV.wc\&wcz}$), shows the melting point in this part is reached before, as the Fig. 4 shows.

Finally, the average temperature of the entire tank (T_{CV}) is lower than the average temperature in the tubes body, due to the effect of the corner and central zones.

It is important to notice that is that average temperatures mask the clear phase change behaviour observed in the individual temperature sensors.
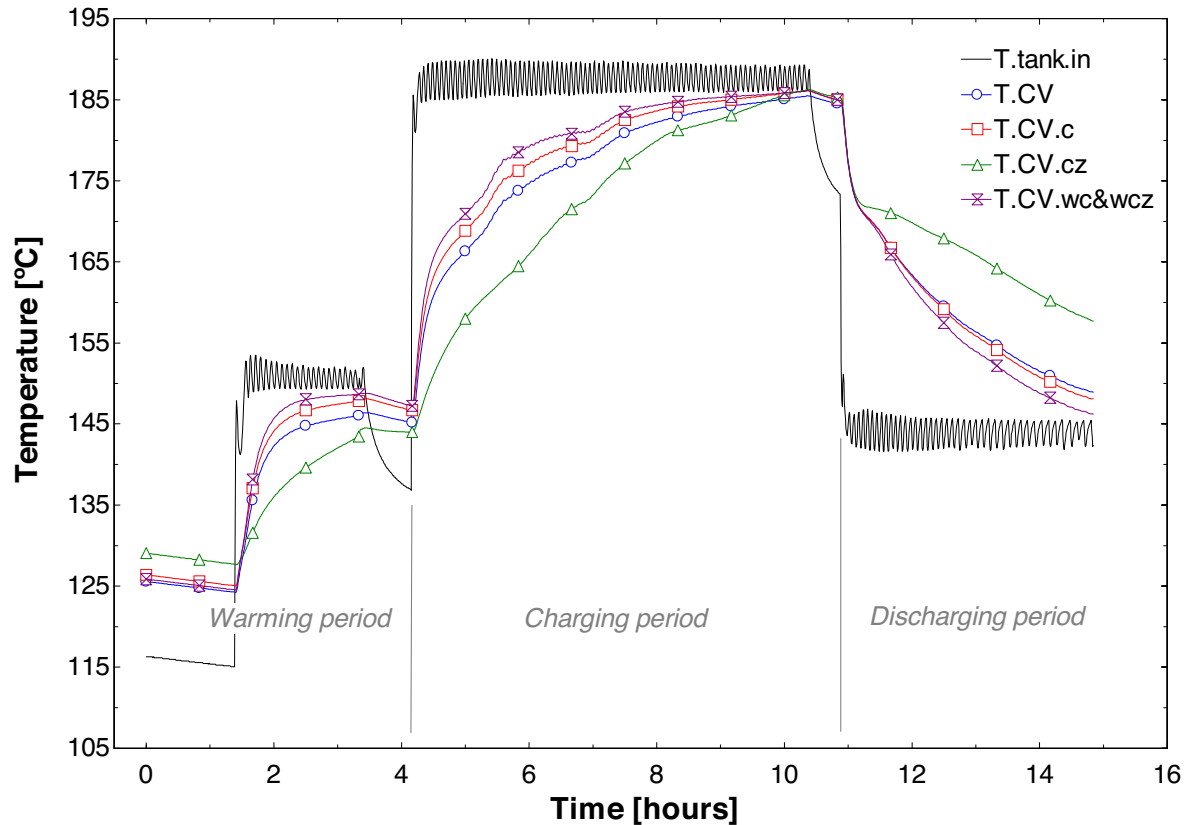

Fig. 5. Calculated average PCM temperatures for the storage tank.

4   Conclusions

This study presents the development of a high temperature thermal energy storage system with latent heat materials at a pilot plant scale. The TES system is targeted for solar cooling applications. To undertake this objective a flexible high temperature pilot plant was built in the University of Lleida.

Research of many candidates as PCM and selection and characterization of the adequate PCM, as well as the design and construction of the TES system were done. Hydroquinone was chosen as the best candidate.

In order to have fast and condensed information about the thermal behaviour of the PCM in the storage tank, average temperatures of the 27 temperatures sensors located in the tank were proposed and compared.

Charging and discharging experiments showed the behaviour of the PCM along the tubes body zone. During the charge, PCM nearest to the HTF inlet reached the melting point before the sensors located farthest (near the HTF outlet).

It was not possible to establish an average temperature representative of the melting state of the PCM, because the melting process was not uniform along the tubes in the tank. The use of the average temperature as indicator of the melting state of the PCM may lead to erroneous conclusions because in reality some parts of PCM are still solid, while other parts are melted. Furthermore, the use of this average temperature for

determining the thermal power to or from the PCM can lead to wrong results. Otherwise, other temperature indicators can be considered to understand the behaviour of separated parts of the tank (corners, central zone, and tubes body).

The average temperature of the tubes body reached the melting point earlier than all the other average temperatures calculated. That is because the HTF transfered the heat better than the other parts of the tank such as corners or central zone. Corners and central zone took longer to reach the melting point due to the low thermal conductivity of the PCM, the longer distance to tubes (HTF) and the proximity to the wall (thermal losses). This effect will be compared with the results obtained in the tank with fins.

5   Acknowledgments

6   References

[1] A. Gil, M. Medrano, I. Martorell, A. Lazaro, P. Dolado, B. Zalba, L.F. Cabeza, RENEWABLE & SUSTAINABLE ENERGY REVIEWS, "State of the art on high temperature thermal energy storage for power generation. Part 1-Concepts, materials and modellization", 14 (2010) 31-55.

[2] M. Medrano, A. Gil, I. Martorell, X. Potau, L.F. Cabeza, RENEWABLE & SUSTAINABLE ENERGY REVIEWS, "State of the art on high-temperature thermal energy storage for power generation. Part 2-Case studies", 14 (2010) 56-72.

[3] A. Gil, P. Arce, J. Roca, M. Medrano, S. Alvarez, L.F. Cabeza, (2009). "Pilot plant for high temperature TES Systems" Proceedings of the11th International Conference of Thermal Energy Storage, Stockholm.

[4] M. Medrano, M.O. Yilmaz, M. Nogues, I. Martorell, J. Roca, L.F. Cabeza, APPLIED ENERGY, "Experimental evaluation of commercial heat exchangers for use as PCM thermal storage systems", 86 (2009) 2047-2055.

[5] MM. Kenisarim, RENEWABLE & SUSTAINABLE ENERGY REVIEWS, "High-temperature phase change materials for thermal energy storage", 14 (2010) 955–970.

[6] B. Zalba, J.M. Marín, L.F. Cabeza, H. Mehling. Review on thermal energy storage with phase change: Materials, heat transfer analysis and applications. Appl Therm Eng, 23 (2003) 251-283.

[7] S.D. Sharma, K. Sagara, Latent heat storage materials and systems: A review. International Journal of Green Energy, 2 (2005) 1-56.

[8] H. Mehling, L.F. Cabeza, (2008). Heat and cold storage with PCM: An up to date introduction into basics and applications. Heat and mass transfer.

[9] C. Castellón, E. Günther, H. Mehling, S. Hiebler, L.F. Cabeza, Determination of the enthalpy of PCM as a function of temperature using a heat-flux DSC—A study of different measurement procedures and their accuracy, International Journal of Energy Research, 32 (2008) 1258–1265.